Differential gain and buildup dynamics of self-starting Kerr lens mode-locked Ti:sapphire laser without an internal aperture

D.-G. Juang, Y.-C. Chen, S.-H. Hsu, K.-H. Lin,* and W.-F. Hsieh

Institute of Electro-Optical Engineering, National Chiao Tung University, Ta-Hsueh Road 1001, Hsin Chu, Taiwan 30050

Received July 24, 1996; revised manuscript received November 1, 1996

The small-signal differential gain was calculated from the measured average cw and Kerr lens mode-locked (KLM) output powers over the least-misalignment-sensitive region of a completely soft-aperturing, self-starting KLM Ti:sapphire laser. The results indicate that the self-starting condition is reached with this laser operating near the center of the stable range. The simulated location of maximum differential gain and pulse buildup process show good agreement with the experimental results. © 1997 Optical Society of America [S0740-3224(97)05007-8]

1. INTRODUCTION

Recently great emphasis has been placed on the use of self-starting Kerr lens mode-locked (KLM) Ti:sapphire lasers without external perturbation elements to achieve broadly tunable short pulses for spectroscopic applications. Using a quantum-well nonlinear reflector in a weakly coupled cavity generated controlled continuously self-starting mode-locked pulses as short as 70 fs in the $TEM_{0,0}$ mode, and the tuning range over which the laser is continuously self-starting is ~30 nm.[1] Constructing an asymmetrical cavity with a slit as a bandwidth-controlling and wavelength-tuning element[2] yielded a self-starting KLM Ti:sapphire laser of pulse width 85 fs at 840 nm; however, self-starting became more and more difficult and was impossible with a wavelength shorter than 815 nm. The self-starting mechanism was attributed to the so-called positive gain-saturation lensing for a laser wavelength longer than the maximum of the gain spectrum.[2] With optimization of the small-signal relative spot size variation due to self-focusing at a hard slit, a self-starting KLM Ti:sapphire laser at 800 nm was demonstrated only in the symmetrical four-mirror confocal cavity configuration.[3,4] However, the maximum value of the hard-aperturing self-starting condition of the laser system is lower than the required theoretical self-starting condition.[3] Thus the self-starting mechanism of KLM solid-state lasers is still a puzzle for ultrashort pulse generation.

We recently demonstrated a self-starting tunable KLM Ti:sapphire laser based on an asymmetrical configuration. This laser can self-start without an internal hard slit and can be tuned over a wavelength range of 780–840 nm while the group-velocity dispersion (GVD) compensation prisms are translated to keep a constant pulse width.[5] The results indicate that gain-saturation lensing is not an essential starting mechanism because KLM can occur with wavelengths shorter than 815 nm, in contrast with Ref. 2. In the present paper, by measuring the average powers of both cw and KLM output, we confirmed not only that the small-signal differential gain estimated from the experimental data indicates that the self-starting condition can be reached but also that the continuously tunable self-starting KLM laser is operated near the center of the low-misalignment-sensitivity (LMS) region,[4] which coincides with the calculated location of maximum saturated differential gain. The optimal cavity design can be achieved to overlap cavity and pump fields by accurate calculation of the astigmatism compensation angle, the position and angle of the pumping lens,[6,7] and GVD compensation.[8] Using iterative simulation, we analyze the buildup process of the KLM Ti:sapphire laser. We find that the pulse is shortened almost monotonically to a few picoseconds, resulting from proper GVD compensation with material dispersion of the rod and not much increase in pulse energy. Then the pulse is further shortened; this is accompanied with increase in pulse energy due to the action of self-phase modulation and the positive saturated differential gain via self-focusing until the laser transits into steady-state mode locking and the pulse width has reduced to the femtosecond regime. The free-running period takes 0.48 ms, which is close to the experimental result of 0.5 ms. However, in the absence of GVD compensation prisms, the pulse-shortening force is weaker, and the KLM pulse is gradually shortened with a continuous increase in pulse energy and takes a longer time to reach steady state, with a final pulse width of 2 ps.

2. EXPERIMENT

Consider an asymmetrical and astigmatism-compensated resonator configuration shown as Fig. 1(a), in which a 2-cm Ti:sapphire rod simultaneously acts as a Kerr medium and a gain medium. To take into account the astigmatism of the Brewster-cut Ti:sapphire rod, the focusing mirrors with radii of curvature of 100 mm were tilted at

0740-3224/97/0802116-06$10.00

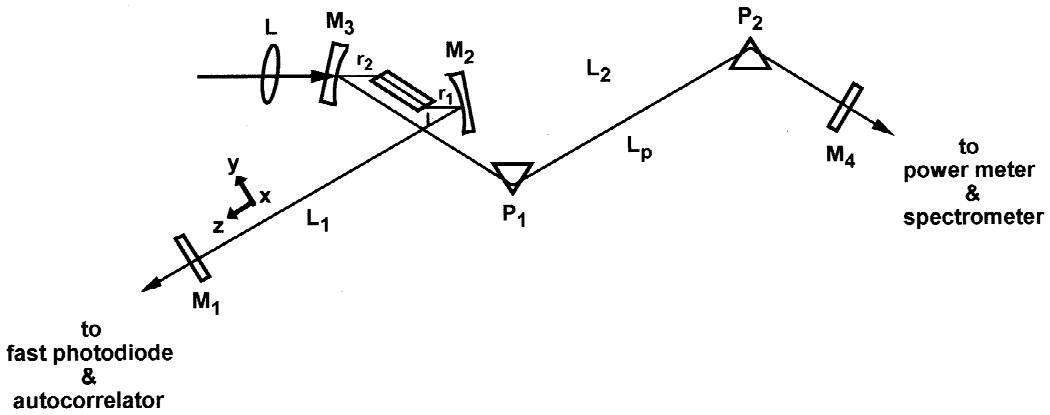

(a)

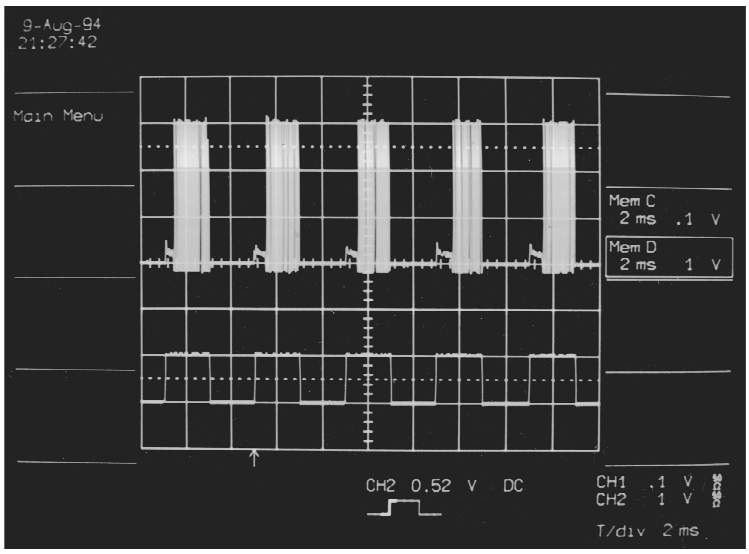

(b)

Fig. 1. (a) Experimental setup for the KLM Ti:sapphire laser. (b) Self-starting self-mode-locked pulse trains monitored by a fast photo diode from M_1.

incidence angles 15° to yield a round $TEM_{0,0}$ mode at 5% output coupler M_1. The focusing-mirror separation is $z_1 = 117.8$ mm, and the distance from one end face of the crystal rod to the focusing mirror M_3 is $r_2 = 47.8$ mm. This cavity corresponds to the configuration located at the center of LMS region.[4] To match both tangential and sagittal KLM beam waists to those of the pump field, this laser is pumped by an all-line Ar-ion laser set at 5-W output power with a pump lens tilted 9° with respect to the incident beam and at a distance of 79 mm from M_3 as in theoretical calculation.[8] Neither a hard-aperture nor a slit was inserted into the cavity. After the GVD compensation SF10 prism pair, was fine tuned,[5] self-starting mode locking was achieved in this soft-aperturing system.

With a mechanical chopper inserted into the cavity, the observed buildup time exhibits wide statistical fluctuation as in Ref. 3. By raising the pump power to 8 W and slightly adjusting prism separation, we obtain the quite reproducible temporal behavior[3,5] of optical pulses shown in Fig. 1(b). The output laser power shows a normal relaxation oscillation followed by short noisy cw steady-state and then turns to KLM pulses once the cavity beam is unblocked. The measured buildup time and pulse duration at M_1 are ~0.5 ms and 150 fs, respectively.[5]

Figure 2 shows the measured cw (solid curve) and KLM (dots) average output powers while the mirror M_2 is continuously moved from $r_1 = 46.5$ to $r_1 = 49.5$ mm. As we change r_1, we do not optimize the rest of the cavity. The solid curve indicates that the cw output power first increases as the mirror M_2 moves closer to M_1 from the far end of LMS (i.e., $r_1 = 49.5$ mm, reaches a maximum at $r_1 \approx 48.5$ mm, then decreases to a minimum at $r_1 \approx 47.75$ mm). It increases again to a maximum and monotonically decreases until the near end of the LMS region is reached. The dotted data represent the output power and range of KLM operation. The self-starting KLM output is located only near $r_1 = 48.0$ mm, which is at the center of the LMS region, and the tunable range is about 300 μm (same as in Ref. 2). The output cw mode is a combination of $TEM_{0,0}$ and the higher-order transverse modes; for instance, the mode pattern at maximum output, where $r_1 \approx 48.5$ mm, consists of 60% $TEM_{0,0}$ and 0.2° off axis 40% $TEM_{0,1}$ modes,[5] whereas the KLM output is a pure $TEM_{0,0}$ mode. Because we have designed

the cavity with proper mirror separation, the beam profile of the KLM mode within the gain medium is always smaller than that of the cw mode, and we have optimized the overlap of beam waists of cavity and pump beams by properly adjusting the tilt angle and distance of the pump lens.[6,7] The minimum cw output power at $r_1 \approx 47.75$ mm is a result of less overlapping between pump and cw $TEM_{0,0}$ modes.

By using a high-Q approximation, which is quite adequate in this laser cavity, one can estimate the small-signal gain g_0 for cw (g_c) and KLM (g_k) modes from the measured output power according to the following equation[9]:

$$I_{\text{out}} = \frac{T_b I_s}{2}\left[T_2\left(\frac{g_0}{L+T} - 1\right)\right], \tag{1}$$

where I_{out} is the measured output intensity, the saturation intensity $I_s = 300$ kW, the transmittance of crystal end faces T_b is set to 1, the transmittance of M_4 is $T_2 = 2\%$, and the total loss $L + T$ is equal to threshold gain. We estimated the small-signal gain difference to be $\Delta g = g_k - g_c = 2 \times 10^{-3}$. To see whether this laser can reach KLM self-starting conditions,[10,11] we set (1) $k/g > \beta\sigma\tau_p$, where k is the differential gain with respect to initial photon flux[10] without taking into account the gain saturation, g is the saturated gain, $\beta = 0.75$ for a Gaussian pulse, the emission cross section σ is 2.7×10^{-19} cm^2, and τ_p is the pulse width; and (2) $\gamma P > T_r/[\ln(m_i)\tau_c]$, where γ is KLM strength[11] corresponding to differential gain for soft aperturing and P is the peak power of the most intensive fluctuation. Assuming that the ratio of the peak power of the most intense fluctuation to the average intracavity power 12 W for round-trip time $T_r = 12.5$ ns, the cavity has $\ln(m_i) \approx 5$–10, and the measured noise bandwidth[12] is 500 Hz for our system, the resulting correlation time is $\tau_c = 0.65$ ms. The result does satisfy both conditions, with, for example, $k/g \approx 5 \times 10^{-29} > 1.5$–$3.0 \times 10^{-30}$. An overestimation may be due to using the small-signal differential gain in the calculation instead of the already saturated differential gain, which is for the case when a cw output is reached before KLM.[5] In Ref. 13 Herrmann derived a necessary and sufficient self-starting criterion from the fluctuation model of the pulse evolution process in mode-locked solid-state lasers. With this criterion the self-starting mode-locking threshold is calculated to be $P_{\text{ml}}/P_{\text{TH}} \geqslant 4$ for our Ti:sapphire laser, where P_{ml} is the pumping and P_{TH} is the lasing threshold. This is fulfilled by either of our experimental setups with $P_{\text{ml}}/P_{\text{TH}}$ approximately 5 and 8.

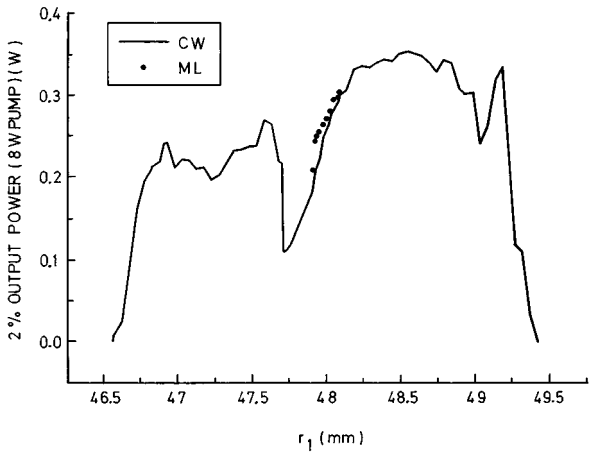

Fig. 2. Measured cw (solid curve) and KLM (dots) average output powers while the mirror M_2 is continuously moved from $r_1 = 46.5$ to $r_1 = 49.5$ mm.

3. THEORETICAL ANALYSIS

Because KLM self-starting depends most critically on the separation of curved mirrors, we are interested in finding the optimal cavity arrangement for mode locking by calculating the saturated differential gain as functions of mirror separation and the buildup process of the KLM laser by seeding an initial pulse train in the cavity after the laser has reached steady-state cw operation. Because the Ti:sapphire crystal is as long as 2 cm, it cannot be treated as a thin medium as in Ref. 14; that is, the spot size and the curvature of phase front varies as functions of position along the optical axis. Thus, the crystal is considered to consist of N slices with thickness $dz = L_c/N$. Each slice can be regarded as a Gaussian duct.[15] Inside each slice the beam radius w, curvature R, and laser power are treated as constants.

The cavity is divided into three regions (as in Ref. 14). Region 1 is a linear propagation from flat mirror M_1 to the crystal surface, and only spatial effects would be considered here; region 2 contains the nonlinear Ti:sapphire crystal with radially varying gain as in Ref. 14, self-focusing, self-phase modulation, and positive dispersion; and region 3 includes elements along the optical path from the crystal surface to the flat mirror M_4, in which both spatial propagation and temporal dispersion compensation were considered.

For a Gaussian pulse the electric field can be expressed as

$$E = \left(\frac{U}{w^2\sigma}\right)^{1/2} \exp\left(-\frac{jkx^2}{2q_x} - \frac{jky^2}{2q_y}\right)\exp\left(\frac{jct^2}{2p}\right), \tag{2}$$

with the spatial q parameter,

$$\frac{1}{q} = \frac{1}{R} - j\frac{\lambda}{n\pi w^2}, \tag{3}$$

and the temporal p parameter,

$$\frac{1}{p} = \frac{2\rho}{c} + i\frac{2}{c\sigma^2}, \tag{4}$$

where R is the phase-front radius of curvature, w is the beam spot size, λ is the central wavelength, n is the refractive index, ρ is the chirping, c is the speed of light, σ is the pulse width, and U is the pulse energy. The transformations of q and p parameters through cavity components can be related by spatial and temporal $ABCD$ matrices[8] as

$$q_{\text{out}} = \frac{Aq_{\text{in}} + B}{Cq_{\text{in}} + D}, \tag{5}$$

$$p_{\text{out}} = \frac{A_t p_{\text{in}} + B_t}{C_t p_{\text{in}} + D_t}. \tag{6}$$

Furthermore, the laser gain equation for time-averaged power in the gain medium is[16]

$$\frac{\mathrm{d}\langle P\rangle}{\mathrm{d}z} = g\langle P\rangle, \tag{7}$$

where the single-pass power gain is

$$g = \frac{4\sigma_0 \tau \alpha_p \lambda_p P_{\text{in}} \exp(-\alpha_p z)}{hc\pi^2 w_{px} w_{py} w_{cx} w_{cy}} Q(z) - \alpha_c, \tag{8}$$

where σ_0, τ, α_p, and α_c are the stimulated emission cross section, the excited-state lifetime, the absorption coefficient at pump wavelength λ_p, and the total cavity loss, respectively. Here w_{px} and w_{py} (w_{cx} and w_{cy}) are radii of the pump beam (cavity beam) in the x and y directions. The overlap integral in Eq. (8) is written as

$$Q(z) = 2\pi \int_{-\infty}^{\infty}\int_{-\infty}^{\infty} \frac{\exp(-A_x x^2 - A_y y^2)}{1 + B\exp(-D_x x^2 - D_y y^2)}\,\mathrm{d}x\mathrm{d}y, \tag{9}$$

with

$$A_x = \frac{2({w_{px}}^2 + {w_{cx}}^2)}{{w_{px}}^2 {w_{cx}}^2}, \qquad A_y = \frac{2({w_{py}}^2 + {w_{cy}}^2)}{{w_{py}}^2 {w_{cy}}^2}, \tag{10}$$

$$B = \frac{2\langle P_+\rangle}{\pi w_{cx+} w_{cy+} I_s} + \frac{2\langle P_-\rangle}{\pi w_{cx-} w_{cy-} I_s}, \tag{11}$$

$$D_x = \frac{2}{{w_{cx}}^2}, \qquad D_y = \frac{2}{{w_{cy}}^2}, \tag{12}$$

where + and − stand for cavity beam propagation in $+z$ and $-z$ directions, respectively. The output power at the ith slice is related to the input power $\langle P_i\rangle$ by

$$\langle P_{i+1}\rangle = \langle P_i\rangle \exp(g\,\mathrm{d}z). \tag{13}$$

In the previous experiment[5] we had observed that the laser underwent transition from relaxation oscillation through a free-running period to Kerr lens mode locking as the pumping beam was turned on. During this period the cw and the KLM modes compete intensively. Finally the laser cavity makes the KLM mode outdo the cw and break into mode-locking operation. The duration of the free-running period and self-starting depends strongly on the alignment and intracavity power. Thus, we calculated the saturated differential gain by seeding a small pulse of intracavity power, $\sim 10^{-6}$ W, in the already saturated free-running laser, rather than calculating the small-signal differential gain, to determine the optimal self-starting cavity configuration. Furthermore, to study the buildup process of the KLM laser, we share some of the cw energy with the pulse mode after the laser has reached steady-state cw, allowing both modes to oscillate simultaneously. An initial pulse is seeded into the cavity at the flat mirror M_4. After a certain round-trip time, one mode will build up to extinguish the other. The principal competition between cw and KLM modes result from gain saturation. The gain saturation term B in Eq. (11) is then modified as

$$B = \frac{2P_{\text{cw}+}}{\pi w_{\text{cw}x+} w_{\text{cw}y+}} + \frac{2P_{\text{cw}-}}{\pi w_{\text{cw}x-} w_{\text{cw}y-}} + \frac{2P_{\text{KLM}+}}{\pi w_{\text{KLM}x+} w_{\text{KLM}y+}} + \frac{2P_{\text{KLM}-}}{\pi w_{\text{KLM}x-} w_{\text{KLM}y-}},$$

where the pumping energy is shared by both modes and w_{cw} and w_{KLM} are beam radii of the cw and the KLM modes, respectively.

We found that the saturated differential gain has less influence on the gain-guiding effect than the small-signal differential gain does (see Ref. 17). Fig. 3(a) shows the saturated differential gain versus the normalized power $K = P/P_c$ (with P_c the self-trapping critical power) for pulses propagating in positive and negative directions, respectively. The resultant differential gain is shown in

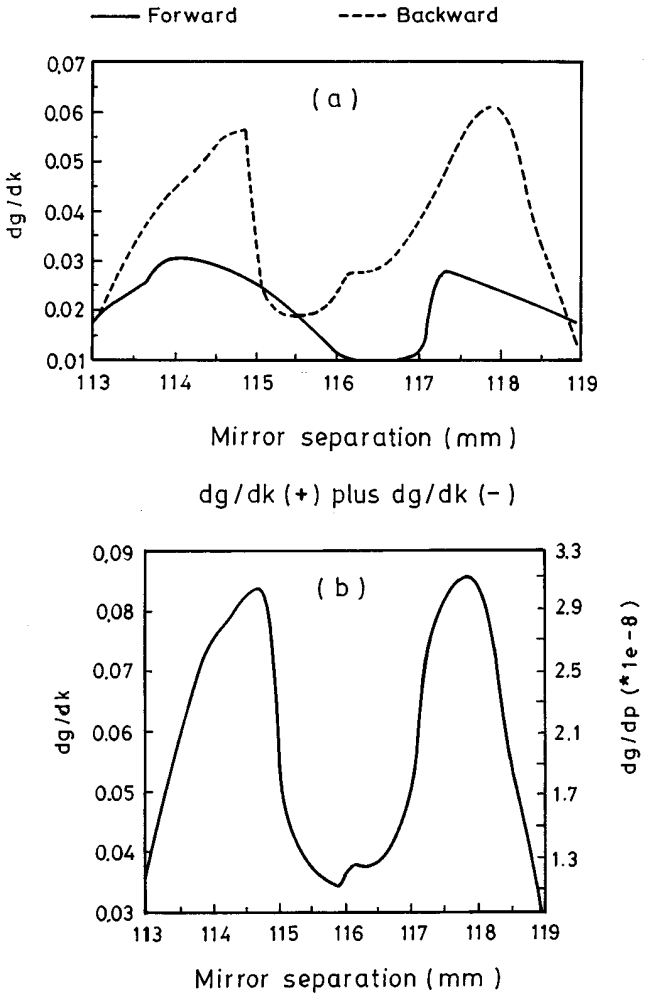

Fig. 3. (a) Differential gain with respect to normalized power K versus mirror separation for pulses propagating in positive and negative directions, respectively. (b) Resultant differential gain. We notice that the largest differential gain for both stable ranges is located near the center of each region.

Fig. 3(b). Note that the largest differential gain for both LMS and high-misalignment-sensitive regions is located near the center of each region and is quite different from hard-aperturing KLM in which the laser operates near the edge of the stable range.[3,4,17] In our calculation we considered only the radially averaged gain. A more precise calculation must consider the power-dependent radiation redistribution, which gives a much stronger differential gain.[18]

Figure 4(a) shows the pulse width and intracavity pulse energy at M_1 versus cavity round-trip time with compensation prisms. Assume that the initial seeding pulse has a pulse width of 10 ps and a peak power 10 times cw average power.[11] We note that the pulse is shortened almost monotonically to 2 ps, resulting from proper GVD compensation with material dispersion of the rod (indeed, it may be accompanied by wavelength shifting[5,19]) until a turning point at approximately the 13000th round-trip where the shortening rate slows down. During this period the pulse energy has not increased much because of a peak power still too low for effective self-focusing to increase pulse gain. Further shortening accompanied by an increase in pulse energy continues owing to the action of self-phase modulation and positive saturated differential gain by self-focusing. Until the 40000th round trip the laser undergoes a transition into steady-state mode locking, and the pulse width is reduced to the femtosecond regime (≈150 fs). The free-running period takes 40000 round trips in our simulation, corresponding to 0.48 ms, which is very close to the experimental result of 0.5 ms. Without the dispersion-compensation prisms as shown in Fig. 4(b), however, owing to a weaker pulse-shortening force in the absence of GVD compensation, the KLM pulse is gradually shortened with a continuous increase of pulse energy and takes ~43000 round trips to reach steady state, when the final pulse width is 2 ps. This result also agrees with our previous result.[12]

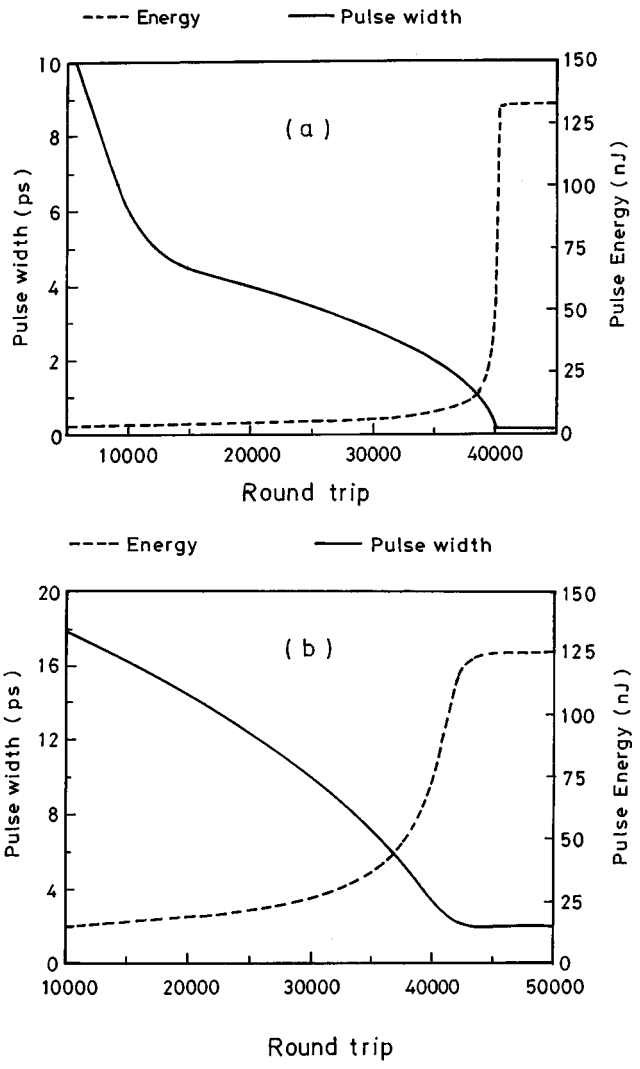

Fig. 4. (a) Pulse width and pulse energy versus cavity round-trip time with compensation prisms; the initial seeding pulse is 10 ps in duration and 1/40 of the cw energy. (b) The buildup of KLM pulses in the Ti:sapphire cavity without dispersion-compensation prisms.

4. CONCLUSIONS

By measuring the average cw and KLM output powers, we have demonstrated that continuously tunable, self-starting, soft-aperturing KLM laser operates at the center of the LMS region. The small-signal differential gain estimated from the experimental data indicates that the self-starting condition can be reached. The simulated result indicates that the largest saturated differential gain for both stable ranges is located near the center of each region and has less influence on the gain-guiding effect. Therefore soft-aperturing KLM is most efficient at this position, consistent with our experimental results. In the buildup studies of this laser, however, we find that the pulse is shortened almost monotonically to a few picoseconds, resulting from proper GVD compensation with material dispersion of the rod with not much increase in pulse energy. Then the pulse is further shortened, accompanied with an increase in pulse energy due to the action of self-phase modulation and positive saturated differential gain by self-focusing until the laser transits into steady-state mode locking and the pulse width has reduced to the femtosecond regime. Without dispersion-compensation prisms, however, due to the weaker pulse-shortening force at the absence of GVD compensation, the KLM pulse is gradually shortened with a continuous increase in pulse energy and takes a longer time to reach steady state. The simulated results agree well with the femtosecond and picosecond experiments.

ACKNOWLEDGMENT

K.-H. Lin is grateful to the National Science Council (NSC) of the Republic of China for providing a fellowship. The research was partially supported by NSC under grant NSC-85-2112-M-009-027.

Correspondence should be addressed to W.-F. Hsieh (e-mail: wfhsieh@cc.nctu.edu.tw).

*Present address: Precision Instrument Development Center, National Science Council, Hsinchu 300, Taiwan.

REFERENCES AND NOTES

1. U. Keller, G. W. 't Hooft, W. H. Knox, and J. E. Cunningham, "Femtosecond pulses from a continuously self-starting passively mode-locked Ti:sapphire laser," Opt. Lett. **16**, 1022 (1991).
2. M. Lai, "Self-starting, self-mode-locked Ti:sapphire laser," Opt. Lett. **19**, 722 (1994).
3. G. Cerullo, S. De Silvestri, and V. Magni, "Self-starting Kerr-lens mode locking of a Ti:sapphire laser," Opt. Lett. **19**, 1040 (1994).
4. G. Cerullo, S. De Silvestri, V. Magni, and L. Pallaro, "Resonators for Kerr-lens mode-locked femtosecond Ti:sapphire lasers," Opt. Lett. **19**, 807 (1994).
5. J.-G. Lai, K.-H. Lin, D.-G. Juang, and W.-F. Hsieh, "Construction of a wavelength-tunable self-starting Kerr lens mode-locked Ti:sapphire laser system," Chin. J. Phys. **34**, 111 (1996).
6. K.-H. Lin and W.-F. Hsieh, "Analytical design of symmetrical Kerr-lens mode-locking laser cavities," J. Opt. Soc. Am. B **11**, 737 (1994).
7. K.-H. Lin, Y.-C. Lai, and W.-F. Hsieh, "A simple analytical method of cavity design for astigmatism compensated Kerr lens mode-locked ring lasers and its applications," J. Opt. Soc. Am. B **12**, 468 (1995).
8. K.-H. Lin and W.-F. Hsieh, "Analytical spatio-temporal design of Kerr lens mode-locked laser resonators," J. Opt. Soc. Am. B **13**, 1786 (1996). Typographical errors were found on p. 1790. In the paragraph below Eq. (33), "σ_1 at output coupler..." should be "σ_1 at M_4…"; in Eq. (35), "$\sigma_1 = \ldots$" should be "$\sigma_1^2 = \ldots$."
9. J. T. Verdeyen, *Laser Electronics*, 3rd ed. (Prentice-Hall, Englewood Cliffs, N.J., 1995), p. 267.
10. E. P. Ippen, I. Y. Liu, and H. A. Haus, "Self-starting condition for additive-pulse mode-locked lasers," Opt. Lett. **15**, 183 (1990).
11. F. Krausz, T. Brabec, and Ch. Spielmann, "Self-starting passive mode locking," Opt. Lett. **16**, 235 (1991).
12. J.-M. Sheih, F. Ganikhanov, K.-H. Lin, W.-F. Hsieh, and C.-L. Pan, "Completely self-starting picosecond and femtosecond Kerr-lens mode-locked Ti:sapphire laser," J. Opt. Soc. Am. B **12**, 945 (1995).
13. J. Herrmann, "Starting dynamic, self-starting condition and mode-locking threshold in passive, coupled cavity or Kerr-lens mode-locked solid-state lasers," Opt. Commun. **98**, 111 (1993).
14. J. L. A. Chilla and O. E. Martínez, "Spatial-temporal analysis of the self-mode-locked Ti:sapphire laser," J. Opt. Soc. Am. B **10**, 638 (1993).
15. A. E. Siegman, *Lasers* (University Science, Mill Valley, Calif., 1986).
16. L. W. Caperson, "Laser power calculations: sources of error," Appl. Opt. **19**, 422 (1980).
17. T. Brabec, Ch. Spielmann, P. E. Curley, and F. Krausz, "Kerr lens mode locking," Opt. Lett. **17**, 1292 (1992).
18. J. Herrmann, "Theory of Kerr-lens mode-locking: role of self-focusing and radially varying gain," J. Opt. Soc. Am. B **11**, 498 (1994).
19. J. Herrmann and M. Muller, "Operating principle, saturable loss, and self-frequency shift in Kerr-shift mode-locked lasers," Opt. Lett. **20**, 22 (1995).